

Article

Development of New Polyimide/Spirulina Hybrid Materials: Preparation and Characterization

Magdalena Aflori , Diana Serbezeanu * , Alina Mirela Ipate, Adina Maria Dobos and Daniela Rusu 

“Petru Poni” Institute of Macromolecular Chemistry, 41A Aleea Gr. Ghica Voda, 700487 Iasi, Romania; maflori@icmpp.ro (M.A.); ipate.alina@icmpp.ro (A.M.I.); necula.adina@icmpp.ro (A.M.D.); rusu.daniela@icmpp.ro (D.R.)

* Correspondence: diana.serbezeanu@icmpp.ro

Abstract: This study presents the synthesis and characterization of polyimide (PI-2) films incorporated with spirulina powder for potential biomedical applications. The synthesis of PI-2 was achieved through a two-step polycondensation reaction using N-methyl-2-pyrrolidone (NMP) as the solvent. The incorporation of spirulina was systematically varied to investigate its effects on the structural and surface properties of the hybrid materials. Scanning electron microscopy revealed a tightly bound interface between spirulina and the PI-2 matrix, indicating effective dispersion and strong interfacial adhesion. Profilometry and Raman spectroscopy confirmed the homogeneous integration of spirulina within the polymer matrix, with resulting variations in surface roughness and chemistry. Contact angle measurements demonstrated altered wettability characteristics, with increased hydrophilicity observed with spirulina incorporation. Furthermore, blood component interaction studies indicated the variations in adhesion behavior observed for red blood cells, platelets, and plasma proteins. Water uptake studies revealed enhanced absorption capacity in PI-2 films loaded with spirulina, highlighting their potential suitability for applications requiring controlled hydration. Overall, this comprehensive characterization elucidates the potential of PI-2/spirulina hybrid materials for diverse biomedical applications, offering tunable properties that can be tailored to specific requirements.

Keywords: polymer hybrid materials; polyimides; spirulina; surface free energy analysis



Citation: Aflori, M.; Serbezeanu, D.; Ipate, A.M.; Dobos, A.M.; Rusu, D. Development of New Polyimide/Spirulina Hybrid Materials: Preparation and Characterization. *J. Compos. Sci.* **2024**, *8*, 178. <https://doi.org/10.3390/jcs8050178>

Academic Editor: Francesco Tornabene

Received: 11 April 2024

Revised: 30 April 2024

Accepted: 9 May 2024

Published: 12 May 2024



Copyright: © 2024 by the authors. Licensee MDPI, Basel, Switzerland. This article is an open access article distributed under the terms and conditions of the Creative Commons Attribution (CC BY) license (<https://creativecommons.org/licenses/by/4.0/>).

1. Introduction

Composite polymers are extensively utilized across diverse industries, encompassing construction (for buildings and bridges), automotive (in manufacturing car bodies), aeronautics (where demand for high-strength, low-density materials is critical), and the production of industrial and residential components (such as storage tanks, bathtubs, washing sinks, and shower stalls) [1–5]. Additionally, composite polymers play a vital role in medical applications [6–11]. Polyimides, characterized by their robust mechanical properties, exceptional thermal stability, and resistance to chemical degradation, have long been heralded as pioneers in material science [12–14]. From spacecraft insulation to microelectronic components, their enduring legacy in high-performance applications is testament to their intrinsic merits. The use of these polymers is, however, restricted by very high melting temperatures. Structural changes to fully aromatic polyimides are often needed to improve machinability, leading to lower melting temperatures and/or improved solubility in organic solvents. An attractive way to achieve these goals is to incorporate bulky side groups along the macromolecular chain. Recently, polyimides have found applicability in the biomedical field [15–18]. Polymer composites, including composite polyimides, represent a class of materials renowned for their exceptional versatility and tailored properties [12,19–25]. Composite polyimides are formed by incorporating reinforcing materials, such as fibers or particles, into a polyimide matrix. This integration endows the resulting material with a unique combination of characteristics, including enhanced

mechanical strength, thermal stability, and chemical resistance. These attributes make composite polyimides highly desirable for a wide range of applications across industries such as aerospace, automotive, electronics, and biomedical engineering. Understanding the fabrication methods, properties, and potential applications of composite polyimides is crucial for advancing materials science and engineering [25–27].

Spirulina is recognized as a source of protein, containing up to 70% protein in dry biomass. In addition to proteins, more than 50 compounds with high biological activity have been described as characteristic of spirulina [28–30]. The immunomodulatory, antimicrobial, antioxidant, anti-inflammatory, and antiviral effects of biomass and spirulina extracts are known. Spirulina (*Arthrospira platensis*) is a species of filamentous cyanobacteria that is used as a food supplement. Due to a high content of proteins and vitamins, spirulina is used as a nutraceutical food supplement, and lately as a raw material for obtaining drugs with multiple health benefits [30–32]. Spirulina may be beneficial in diseases that are known to be aggravated by reactive oxygen species and in the development of new treatments for neurodegenerative disorders, such as Alzheimer's or Parkinson's disease [33,34]. The spirulina presented in its structure several organic functional groups, such as hydroxyl from polysaccharides and carboxyl from proteins [32]. The protein in *Spirulina* sp. is the blue pigment phycocyanin, a protein composed of a collection of peptides that form polypeptides, with each peptide being composed of amino acids containing a carboxyl group [35]. Besides carboxyl groups, phycocyanin also consists of carbonyl groups, amines, amides, phosphoryl, and sulfonyl [35]. The phycocyanin is mostly used for its anti-oxidant, anti-cancer, and anti-inflammation properties [36]. Spirulina–polymer composites form a relatively new subject of study, mainly used for tissue engineering scaffold [37,38], but due to the unique properties of the components, other application areas can be discovered. Given the above, it is intriguing to combine the properties of polyimides with those of spirulina to create a new material for potential use in various medical applications. In this sense, polyimide films containing different amounts of spirulina were obtained.

Therefore, to address this objective, the initial approach involved incorporating spirulina into the polyimide matrix synthesized from 2,2-bis(4-(4-aminophenoxy)phenyl)propane and 4,4'-oxydiphthalic anhydride. Additionally, polyimide films with varying concentrations of spirulina powder were examined through profilometry, Raman spectroscopy, contact angle measurements, and water absorption studies. The refinement stages of the chemical composition of selected polymeric materials, along with optimization processes to achieve uniform film properties, must consider the specific requirements of the intended applications. Furthermore, a comprehensive characterization of these polymeric materials was conducted.

2. Materials and Methods

2.1. Materials

2,2-bis(4-(4-aminophenoxy)phenyl)propane, 4,4'-oxydiphthalic anhydride, and N-methyl-2-pyrrolidone were purchased from Merck (Darmstadt, Germany). Spirulina powder was purchased from Springmarkt (Adams Vision S.R.L., Târgu Mureș, str. Hunedoara 31, Romania). Other reagents used in this study were bought from commercial sources and were used as received or were purified using various standard methods.

2.2. Synthesis of PI-2

Polyimide PI-2 was synthesized through a two-step polycondensation reaction of the diamine 2,2-bis(4-(4-aminophenoxy)phenyl)propane, with the commercially available aromatic dianhydride 4,4'-oxydiphthalic anhydride, using NMP (N-methyl-2-pyrrolidone) as the solvent (Figure 1). The viscous solution obtained was subjected to cyclodehydration by heating at 180 °C under a gentle stream of nitrogen for 24 h. After cooling to room temperature, the solution was diluted by adding NMP and precipitated in distilled water. The resulting polymeric powder was collected using vacuum filtration and then washed repeatedly with distilled water. Polymer purification was achieved through Soxhlet

extraction in ethanol to remove unreacted monomers and residual non-volatile solvent. Subsequently, the sample was dried in an oven at 100 °C under vacuum for 12 h.

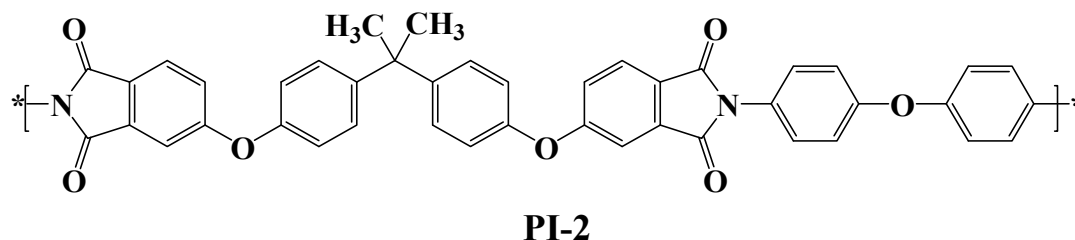


Figure 1. Chemical structure of the PI-2.

The structure of the obtained polymer was investigated through absorption spectroscopy in FTIR (Fourier-transform infrared spectroscopy) and ¹H NMR (proton nuclear magnetic resonance). The most significant signals in the FTIR spectra of polymer PI-2 are presented in Table 1.

Table 1. Absorption bands of polymer PI-2.

Polymer	Absorption Bands						
	Ar. C–H, ν	Alif. C–H, ν	Ar. C=C, ν	Imide C=O, ν	Imide C–N, ν	Imide C=O, δ	Ar. C–O–C, ν
PI-2	3063	2938	1603 1505	1778 asymm. 1720 symm.	1368	744	1240

Ar. Aryl; ν vibrational frequency; δ deformation vibration; alif. aliphatic; asymm. asymmetric stretch or deformation; symm. symmetric stretch or deformation.

2.3. Films Preparation

A measure of 1 g of polyimide PI-2 was dissolved in 10 mL NMP at room temperature. A measure of 2 mL was taken from the stock solution, over which different amounts of spirulina were added. The PI-2/spirulina hybrid materials were prepared by pouring the mixed solutions into Petri dishes and heating them to 50 °C (30 min) and 100 °C (2 h), respectively, with the aim of removing the solvent. The concentration of spirulina in the final solution was 5%, 10% and 20%, respectively.

2.4. Methods

2.4.1. FTIR

The infrared spectra of the films were achieved with a Bruker LUMOS—FTIR Microscope spectrometer (BrukerOptik GmbH, Ettlingen, Germany) equipped with an ATR reflection module (attenuated total reflection), a crystal of diamond and OPUS 8 software (Version 8, Ettlingen, Germany). Additionally, a single reflection at a 45° angle was used for spectral processing. The scan interval used for each sample ranged between 600 and 4000 cm^{−1}. Our samples with plant extract were registered in a transmission module. All the spectra were scanned at a temperature of 25 °C.

2.4.2. ¹H NMR Spectroscopy

The ¹H NMR spectra of optimized polymer matrices were recorded in DMSO-d₆ at 25 °C using a Bruker Avance DRX 400 spectrophotometer (Rheinstetten, Germany).

2.4.3. Scanning Electron Microscopy (SEM)

The morphology of the films investigated in this study (PI-2 and PI-2/S(1–3)) was highlighted by scanning electron microscopy, using a Quanta 200 ESEM device that stops at

25 KV. Before the analysis, the samples were covered with a fine layer of gold by spraying (EK 3135 EMITECH).

2.4.4. Profilometry

The surface topography of the films was studied with an Alpha-Step D-500 Tencor stylus. The arithmetical mean surface roughness values (Ra) were estimated from an average of five profiles (KLA Tencor Corporation, Milpitas, CA, USA). The profiler estimates the parameters of roughness using a speed of 0.10 mm/s and an interval of filtration of 0.060 mm. The accuracy used for estimating the parameters of roughness ranged from 10 Å to 1.2 mm. Five profiles were recorded for each sample and the surface roughness was measured in nm.

2.4.5. Raman Microscopy

A confocal Raman microscope spectrometer (Renishawplc, Gloucestershire, UK) was utilized to record some images using a Leica DM2700 microscope. This microscope has different objectives, such as 5×, 20×, 50× and 100×. The spectrometer is equipped with a Renishaw Depletion Deep CCD Centrus array detector. The excitation laser has a line of detection at 633 nm.

2.4.6. Contact Angles

In order to record the surface free energy of our films, the contact angle was determined using the technique with the statistic drop. A goniometer KSV CAM 101 was used with an optical system and a camera CDD connected to an electronic device. A Hamilton syringe was used to place each sample on a special substratum plate with ~1 µL of liquid. All the recorded images were transmitted through a CDD camera for analysis. The static contact angle was obtained from the interface liquid/solid and the interface liquid/vapor. Through all the experiments, a constant moisture and temperature was registered (25 °C and 65%, respectively). The results were made three times and the mean ± standard deviation was established.

2.4.7. Water Absorption

Thus, the wetting capacity of these films was investigated, determined primarily by the type of polyimide involved and the predominant ambient humidity. For the studied films, dimensions within 0.5 × 0.5 cm² were chosen. These samples were immersed in 10 mL of Milipore water at 37 °C for different periods of time. Then, the samples were removed and the excess water from the surface was quickly removed with the help of filter paper. Thus, the films were weighed dry and then at different time periods. The degree of swelling was determined using the calculation formula:

$$W(\%) = \frac{W_t - W_d}{W_d} \times 100 \quad (1)$$

where W (%) is the amount of water absorbed; W_d is the dry weight of the polymer; and W_t is the weight of the hydrated polymer. The experiments were conducted in triplicate, and the mean ± standard deviation was calculated from the results obtained.

2.4.8. Statistical Analysis

The results are expressed as the mean ± standard deviation (SD) of at least three replicates. Statistical significance (5%) was evaluated with one-way analysis of variance (ANOVA) followed by Student's t -test $p < 0.05$. All statistical analysis was performed using OriginPro 2018 software (OriginLab Corporation, Northampton, MA, USA).

3. Results and Discussions

3.1. Fourier-Transform Infrared with Attenuated Total Reflectance Spectroscopy (FTIR-ATR) Analysis

The chemical structure of the investigated samples was elucidated using FTIR spectroscopy. Figure 2 shows the FTIR spectra for the films marked PI-2 and PI-2/S(1–3). In the FTIR spectra of the polymers PI-2 and PI-2/S(1–3), strong absorption bands appeared at $1780\text{--}1770\text{ cm}^{-1}$ and $1730\text{--}1720\text{ cm}^{-1}$ attributed to the asymmetric and symmetrical elongation vibrations of the carbonyl group in the imide ring and carbonyl ester. The region $1730\text{--}1720\text{ cm}^{-1}$ should have two peaks representative of the carbonyl groups in the imide rings and the ester groups. The absorption band at 1380 cm^{-1} was due to the elongation vibrations of the C–N group in the imide ring, and the absorption band at 724 cm^{-1} was due to the deformation vibrations of the imide ring. Absorption bands also appear at 3070 cm^{-1} and 1602 cm^{-1} , being characteristic for the aromatic C–H connection and aromatic C=C. The FTIR analysis of spirulina reveals characteristic peaks associated with proteins, such as the amide bands Amide I ($\sim 1650\text{ cm}^{-1}$), Amide II ($\sim 1540\text{ cm}^{-1}$), and Amide III ($\sim 1230\text{ cm}^{-1}$), corresponding to C=O stretching, N–H bending, and C–N stretching vibrations, respectively [35]. Carbohydrates, including polysaccharides like glycogen, are also present, exhibiting FTIR peaks related to C–O stretching and bending vibrations ($\sim 1200\text{--}1000\text{ cm}^{-1}$) [29]. Lipids in spirulina, encompassing fatty acids and glycolipids, manifest FTIR peaks primarily at $\sim 3300\text{--}2925\text{ cm}^{-1}$ (CH_2 and CH_3 stretching) and $\sim 1645\text{ cm}^{-1}$ (C=O stretching in ester groups of triglycerides). Furthermore, spirulina harbors pigments like chlorophylls and carotenoids, with carotenoids displaying peaks at around $1500\text{--}1600\text{ cm}^{-1}$ (C=C stretching). While minerals and trace elements contribute to spirulina's nutritional profile, their detection via FTIR may be limited, although certain functional groups associated with minerals may be indirectly observed. After normalization to the 1602 cm^{-1} band characteristic for the connection of aromatic $\delta_{\text{C-H}}$ and aromatic $\nu_{\text{C=C}}$ from PI-2, an increase in the integrated area of the peak between 1697 and 1660 cm^{-1} could be observed. This indicates an increased interaction of spirulina with polyimide in the structure of composite samples with an increased amount of spirulina. These vibrations are specific for protein groups ($\nu_{\text{C=O}}$ stretch bands (asymmetric) corresponded to the carbonyl groups (C=O) of the primary protein amides, while at 1400 cm^{-1} (symmetrical) for the carboxylate ions present in spirulina). The band at 1540 cm^{-1} from the protein secondary amides (–NH), present in composite samples, is very weak but visible [35].

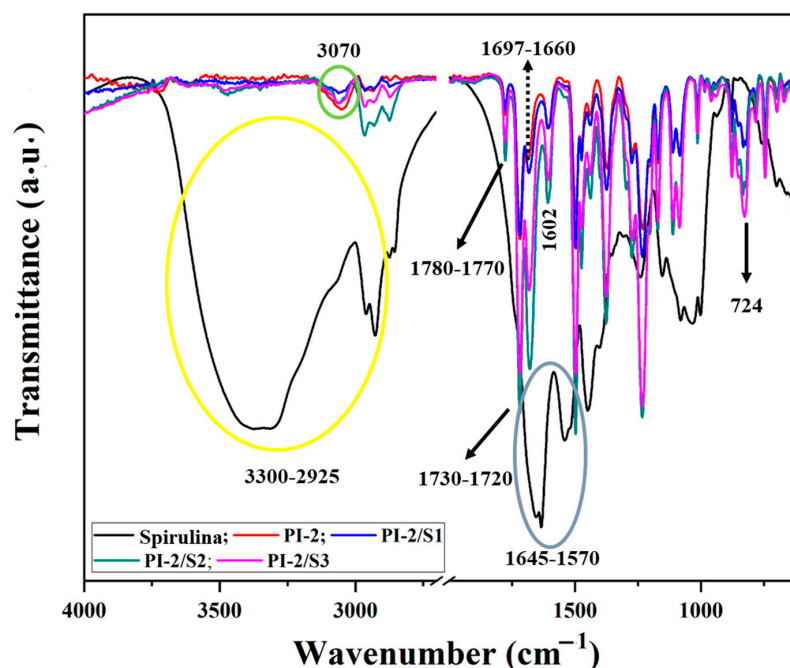


Figure 2. FTIR spectrum of PI-2 and PI-2/S(1–3) polyimide film.

3.2. Surface Morphology and Surface Roughness Analysis of Films

Figure 3 provides insight into the fracture morphologies of PI-2 films with varying loading contents of spirulina. Notably, Figure 3b–d exhibit a tightly bound interface between spirulina and the PI-2 matrix, characterized by a distinct absence of cavities and agglomeration of spirulina particles. The effective dispersion of spirulina within the PI-2 matrix is a pivotal factor in enhancing the performance of polyimide-based composites, particularly in biomedical applications. PI films offer a range of desirable properties for such applications, including excellent mechanical strength, chemical resistance, and biocompatibility [15–18]. When incorporating spirulina into the PI matrix, ensuring uniform dispersion throughout the composite is crucial for optimizing its properties and functionalities. This uniform dispersion facilitates the integration of spirulina's nutritional components, such as proteins, carbohydrates, lipids, and pigments, into the composite structure, thereby potentially enhancing its biocompatibility and bioactivity. Additionally, the absence of cavities within the composite is advantageous for biomedical applications due to several reasons. Firstly, cavities or voids can serve as potential sites for microbial growth, which can compromise the biocompatibility and sterility of the composite, especially in medical implant applications. Secondly, void-free structures improve the mechanical integrity and durability of the composite, ensuring its long-term performance in biomedical settings. Therefore, by effectively dispersing spirulina within the PI-2 matrix and minimizing the presence of cavities, polyimide-based composites can offer enhanced properties and functionalities suitable for various biomedical applications. Overall, the versatility of polyimide films makes them valuable materials for a wide range of biomedical applications, spanning from implantable devices and drug delivery systems to biomedical sensors, microfluidic devices, tissue engineering scaffolds, and flexible electronics. Their biocompatibility, mechanical properties, and tunable surface characteristics make them indispensable for advancing healthcare and biomedical research. This observation aligns with the growing interest in bio-inspired materials for biomedical applications, where natural compounds like spirulina are utilized to impart desirable properties to synthetic matrices, as evidenced by recent studies. The absence of cavities suggests strong interfacial adhesion between spirulina and the polyimide matrix, indicating a robust interaction that enhances the mechanical integrity of the hybrid materials. This cohesive interface is essential for maintaining the structural integrity and stability of the composite, particularly under mechanical stress or in physiological environments. Furthermore, the lack of agglomeration indicates uniform dispersion of spirulina throughout the polyimide matrix. This uniform distribution is advantageous for achieving consistent and predictable properties in the composite material, such as mechanical strength, thermal stability, and bioactivity. Moreover, the uniform dispersion of spirulina enhances its accessibility for potential biological interactions, facilitating the release of bioactive compounds and promoting therapeutic efficacy in biomedical applications. Overall, the tight binding interface and the absence of cavities or agglomeration observed in Figure 3b–d highlight the successful integration of spirulina into the PI-2 matrix, paving the way for the development of polyimide-based hybrid materials with enhanced functionality and biocompatibility for various biomedical applications.

Profilometry and Raman spectroscopy techniques were employed to meticulously examine the surface characteristics of the films, aiming to underscore the homogeneous integration of spirulina powder within the PI-2 polymer matrix (Figure 4). Furthermore, these analyses sought to pinpoint the optimal composition essential for refining and validating a novel experimental model. Topographical and morphological features serve as pivotal parameters in delineating the properties of resultant materials, along with their influence on cellular adhesion to the polymeric substrate. The roughness parameters, namely Ra (Arithmetic mean roughness) and Rq (Square average roughness), of the optimized films were meticulously analyzed. Across various compositions of polyimides with or without different spirulina ratios, Ra roughness values fell within the range of 2.15–33.4 nm (Table 2), while Rq roughness ranged from 4.08 to 49.3 nm (Table 2). These values underscore the intricate interplay between surface topography and spirulina incorporation within

the polymer matrix. The novel compositions of the film surface exhibited a discernible modification in surface roughness, a crucial characteristic influencing the incorporation and stabilization properties of phytotherapeutic agents. This nuanced adjustment in roughness parameters not only reflects the meticulous optimization efforts but also holds significant implications for the overall performance and efficacy of the resulting composite materials in biomedical applications.

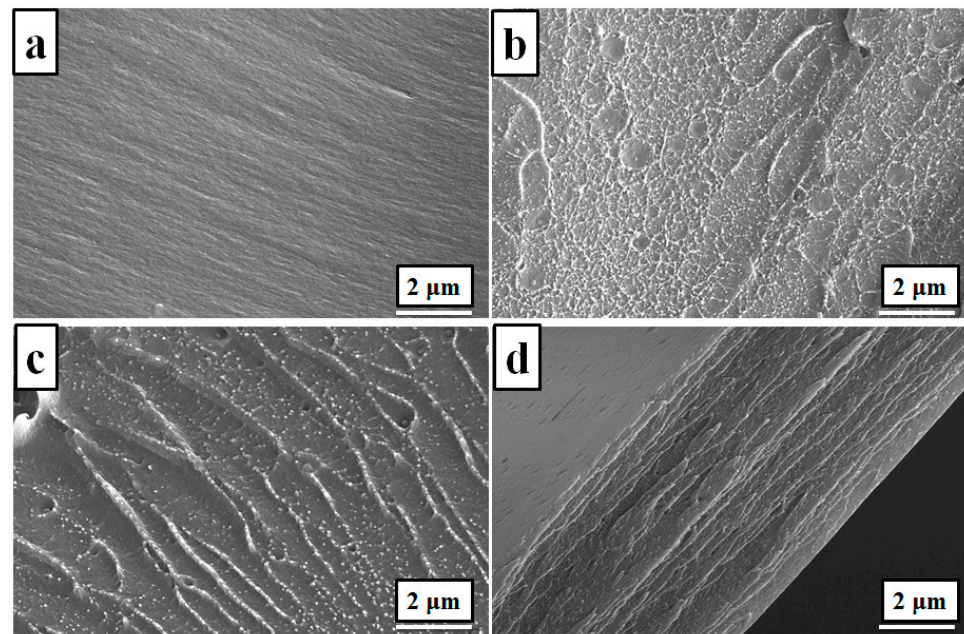


Figure 3. SEM images of the PI-2 (a), PI-2/S1 (b), PI-2/S2 (c), and PI-2/S3 (d) hybrid materials at a magnitude of 10,000 \times .

Table 2. Values of the parameters Ra and Rq for the optimized films PI-2 and PI-2/S(1–3) hybrid materials.

Sample	Roughness	
	Ra * (nm)	Rq ** (nm)
PI-2	2.150	4.087
PI-2/S1	11.82	18.59
PI-2/S2	20.08	32.16
PI-2/S3	33.44	49.32

* Ra: Arithmetic Average Roughness; ** Rq: Root Mean Square Roughness.

The complementary use of Raman spectroscopy alongside SEM imaging fortifies our understanding of the structural and chemical composition of the samples under investigation. The congruence between the observations derived from SEM images and the findings obtained through Raman spectroscopy is instrumental in corroborating and enhancing the comprehensiveness of our analysis. In particular, the SEM images provide valuable insights into the physical morphology and spatial distribution of the constituents within the samples. Conversely, the confirmation provided by the Raman figures aligns with the SEM observations, thereby validating the uniform incorporation of spirulina powder within the PI-2 polymer matrix. This confluence of evidence underscores the robustness and reliability of our characterization approach, facilitating a comprehensive understanding of the complex interplay between material structure, composition, and functionality.

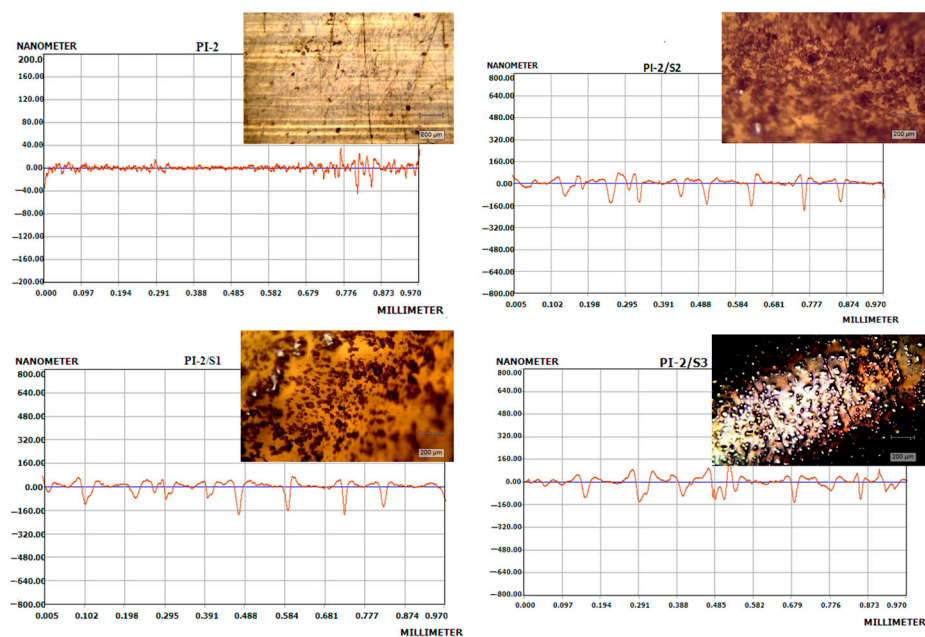


Figure 4. Surface morphology and surface roughness analysis of PI-2/S(1–3) hybrid materials.

3.3. Contact Angle and Surface Free Analysis of Film

The optimization of the composition of the PI-2 film in which the spirulina powder was successfully incorporated was made from the point of view of the wettability properties. To analyze the hydrophobic/hydrophilic character of PI-2 and PI-2/S(1–3) hybrid materials, static contact angle measurements were performed. In this sense, three different liquids were used to determine the contact angle, namely distilled water (W), diiodomethane (CH_2I_2) and ethylene glycol (EG). From Figure 5, it can be seen that the contact angles between the polymeric surfaces and the drops change as a result of the influence of structural features (monomers used in synthesis, the interaction between polymer and solvent used, the interaction between polymer used and spirulina, and the orientation effect of macromolecular chains after thermal imidization) but also because of the surface tension of the liquid test used and forces that they generate at the interface with the polymeric substrate. The water, diiodomethane and ethylene glycol absorption characteristics of the different polyimide–spirulina hybrid materials (PI-2/S1, PI-2/S2, and PI-2/S3) were systematically investigated in comparison to the pure polyimide film (PI-2). The results reveal a notable trend in water absorption, with a consistent increase observed as the content of spirulina increases and water contact angle values decrease. Specifically, PI-2/S3 exhibited the highest water absorption, with a contact angle of 51.12, showcasing the potential of spirulina incorporation in increasing the wettability.

According to the literature [39,40], the values for water contact angles varying between $10^\circ < \theta < 90^\circ$ are characteristic for hydrophilic samples, while those ranging in $90^\circ < \theta < 150^\circ$ denote hydrophobic surfaces. Thus, the polyimide film has a hydrophobic character with a water contact angle of approximately 90° . With the addition of spirulina in different amounts, a decrease in contact angles is observed, which shows that the samples become hydrophilic. The obtained results are in agreement with the literature data according to which spirulina has a large proportion of hydrophilic sites for binding water molecules [41]. Therefore, an increase in spirulina amount will generate an increase in the number of these sites for fixing water molecules.

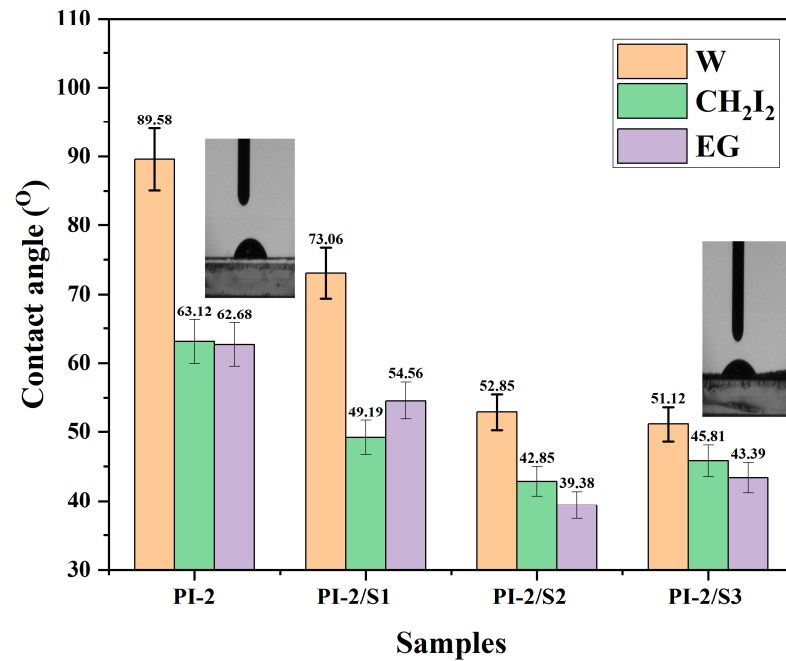


Figure 5. Graphical representation of contact angle values for PI-2 and PI-2/S(1–3) films; CH₂I₂ drop images from the contact angle measurements for the PI-2 and PI-2/S3 hybrid materials.

Contrastingly, the diiodomethane and ethylene glycol absorption data present a more complex picture. Thus, PI-2/S1 and PI-2/S2 absorb the drops of the two liquids more easily compared to PI-2, while PI-2/S3 demonstrated a slight decrease in absorption demonstrated by an increase in the contact angle values. This statement is also supported by the values of the surface tension parameters. These parameters are obtained by applying mathematical approximations and help in establishing the hydrophilic/hydrophobic character of the sample. Therefore, the acid/base method (LW/AB), Equations (2)–(4) [42], implies that the contact angle values (Figure 5) measured between the solid surface and drops of the used liquid, and also the surface tension parameters of test liquids (Table 3), were applied [42–48].

$$1 + \cos \theta = \frac{2}{\gamma_{lv}} \cdot \left(\sqrt{\gamma_{sv}^d \cdot \gamma_{lv}^d} + \sqrt{\gamma_{sv}^+ \cdot \gamma_{lv}^-} + \sqrt{\gamma_{sv}^- \cdot \gamma_{lv}^+} \right) \quad (2)$$

$$\gamma_{sv}^p = 2 \cdot \sqrt{\gamma_{sv}^+ \cdot \gamma_{sv}^-} \quad (3)$$

$$\gamma_{sv} = \gamma_{sv}^d + \gamma_{sv}^p \quad (4)$$

where “ θ ” represent the contact angle between the polymeric surface and drop of the test liquid, subscripts “lv” and “sv” refer to the liquid–vapor and surface–vapor interfacial tension, respectively, while “p” and “d” are superscripts indicating the polar and disperse components of the total surface tension “ γ_{sv} ”.

As data obtained show (Table 3), for all samples, that the disperse components, γ_{sv}^d , are always higher than the polar ones, γ_{sv}^p , while the electron acceptor parameter, γ_{sv}^+ , is smaller than the electron donor parameter, γ_{sv}^- . However, analyzing according to the content of spirulina added to the PI-2 sample, it is observed that the polar component increases with the increase in the spirulina content, which means an improvement in the sample’s hydrophilicity. This happens up to a critical spirulina content of 10%, after which a slight decrease is observed.

Table 3. Surface tension parameters of the liquids used, blood components and plasma proteins for contact angle measurements [42,44–49].

Liquid	γ_{lv}	γ_{lv}^d	γ_{lv}^p	γ_{lv}^+	γ_{lv}^-
Water (W)	72.8	21.8	51.0	25.5	25.5
Ethylene glycol (EG)	48.0	29.0	19.0	1.92	47.0
Diodmethane (CH ₂ I ₂)	50.8	50.8	0.0	0.72	0
Biological material					
Red blood cell	36.56	35.20	1.36	0.01	46.20
Platelet	118.24	99.14	19.10	12.26	7.44
Albumin	62.50	26.80	35.70	6.30	50.60
Fibrinogen	41.50	37.60	3.89	0.10	38.00
IgG	51.30	34.00	17.30	1.50	49.60

Knowing the surface free energy also helps in establishing the hydrophilic/hydrophobic character of the samples. This parameter was determined by applying Equation (5) [42], with and from Table 4 and Figure 5, respectively.

$$\Delta G_w = -\gamma_{lv} \cdot (1 + \cos \theta_{water}) \tag{5}$$

Table 4. Surface tension parameters γ_{sv}^d , γ_{sv}^p (mN·m⁻¹) and contribution of the polar component (γ_{sv}^+ , γ_{sv}^-) to the total surface tension, γ_{sv} , for films obtained from PI-2/spirulina mixture according to the acid/base method (Equations (2)–(4)).

Sample	Acid/Base Method				
	γ_{sv}^d	γ_{sv}^p	γ_{sv}^+	γ_{sv}^-	γ_{sv}
PI-2	24.52	3.12	0.72	3.36	27.64
PI-2/S1	29.62	3.74	0.25	14.30	33.36
PI-2/S2	30.16	8.42	0.54	33.07	38.58
PI-2/S3	28.21	7.70	0.39	38.44	35.91

The variation in ΔG_w as a function on the water contact angle, θ_{water} , is represented in Figure 6.

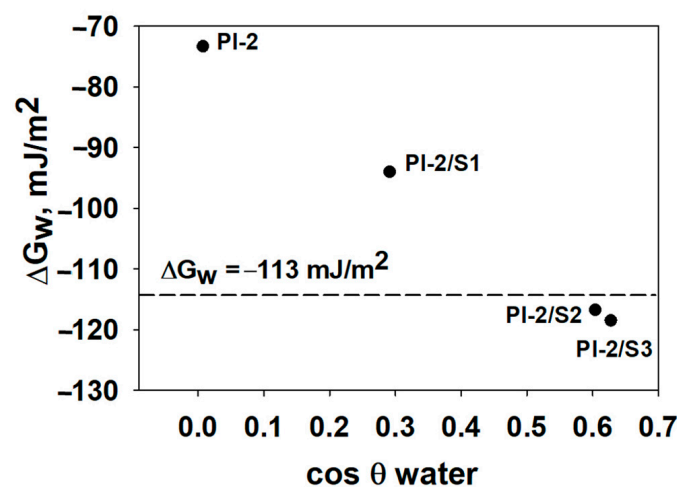


Figure 6. Dependence of the surface free energy function of water contact angle for PI-2/spirulina hybrid materials.

In the literature, it is specified that a value of $\Delta G_w < -113$ corresponds to a hydrophilic surface, while values of $\Delta G_w > -113$ correspond to hydrophobic ones [50]. As can be observed from Figure 6, samples with the highest spirulina contents are hydrophilic compared to the one containing a small amount or pure polyimide sample. This means that the addition of spirulina has a significant role in improving the hydrophilicity of polyimides.

There are numerous studies that correlate the morphology and topography of polymeric surfaces with the wetting properties. In some of them, the increase in roughness leads to an increase in hydrophobicity, while in others the rough surfaces are presented as hydrophilic [51,52]. In the present study, the addition of spirulina in different ratios leads both to a change in the chemistry of the studied surfaces and also to an increase in their roughness, as can be seen from the data listed in Table 2. These factors will lead to a significant decrease in the values of the contact angle and implicitly towards more hydrophilic surfaces. This is in agreement with the literature data according to which a rough surface will enhance the wettability caused by the chemistry of the surface [53]. In conclusion, the variations regarding the surface properties of the analyzed films suggest that the incorporation of spirulina can influence the material's interaction with different test liquids, emphasizing the importance of tailoring compositions for specific applications. In summary, the observed water, diiodomethane, and ethylene glycol absorption trends underscore the versatility of these polyimide–spirulina hybrid materials, offering tunable properties that can be tailored for diverse applications as materials with controlled solvent permeability. The findings provide valuable insights for further optimizing these hybrid materials based on specific performance requirements.

3.4. Polyimide/Spirulina Hybrid Materials—Blood Component Interaction

For the analyzed materials to be applied in the biomedical field, first of all, they must be biocompatible and, secondly, present antimicrobial activity. The surface of a material is the first component of an implant that comes into contact with cells or biological fluids. Usually, the biocompatibility is given by the surface characteristics of the material, especially by wettability, surface chemistry and surface topography. In the present paper, a mathematical approximation was used (Equation (6)) [49] that, together with the parameters outlined above, can make a prediction regarding the biocompatibility of materials based on polyimides/spirulina. Compatibility with blood refers to the way in which the polymeric material behaves when it comes into contact with all its components, namely: red blood cells (rbc), platelets (p), and plasma proteins (albumin, immunoglobulin G (IgG), and fibrinogen). In this sense, determination of the spreading work of blood components and plasma proteins over the polymeric surfaces by using surface tension parameters listed in Tables 4 and 5 was necessary. Data obtained are listed in Table 5.

$$W_s = W_a - W_c = 2 \cdot \left(\sqrt{\gamma_{sv}^{LW} \cdot \gamma_{lv}^d} + \sqrt{\gamma_{sv}^+ \cdot \gamma_{lv}^-} + \sqrt{\gamma_{sv}^- \cdot \gamma_{lv}^+} \right)^{1/2} - 2 \cdot \gamma_{lv} \quad (6)$$

where W_s represents the work of spreading and is given by the difference between the work of water/blood component adhesion, W_a , and work of water/blood component cohesion, W_c .

It is known from the literature that red blood cells and platelets decide the lifetime of an implanted polymeric material. These components, through their adhesion to the material surface, can cause coagulation with a major impact on thrombogenicity and immunogenicity. In this context, it can be stated that the adhesion of red blood cells can be used as a parameter that characterizes the biomaterial function on cell adhesion. The polymeric materials with a lower work of adhesion will have a lower extent of cell adhesion compared with those with a higher work of adhesion [54]. As can be seen from Table 5, the work of spreading for red blood cells and platelets takes negative values, which means that $W_c > W_a$ in the case of both types of cells. However, the spreading work obtained for red blood cells is higher compared to that obtained for platelets, indicating an essential role in

blood coagulation. For platelets, which are essential in maintaining hemostasis, negative values of the spreading work were recorded, which means a lower work of adhesion, comparatively with the one of cohesion. In the literature [55], it is maintained that platelet aggregation is used as an indicator for the material's thrombogenic features, so knowledge of the surface polymer–platelet interaction is an important step towards the understanding and establishment of the hemocompatibility. Thus, the negative values of the spreading work of platelets (Table 5) indicate that polyimide/spirulina hybrid materials present a pronounced cohesion. This means that polymers do not interact with platelets, thus preventing their adhesion and activation of coagulation at the blood–biomaterial interface.

The slightly higher values obtained for fibrinogen spreading work show that the studied materials can be successfully used as biomaterials because they can prevent the excess deposition of red blood cells. For albumin and IgG, the obtained values reveal that cohesion prevails, which is characteristic of nonabsorbent behavior, as required by bio-applications. In the current study, for both plasma proteins (albumin and IgG), the work of spreading varies in the same way, namely, it increases with the addition of spirulina, up to a critical content of 10%, after which a slight increase in cohesion is noted. The adsorption of plasma proteins is difficult to analyze due to the many factors involved. In this context, as previously mentioned, the composition [56], hydrophilic/hydrophobic [57] character, and electrical potential, known as the zeta potential [58], are factors with a major impact on the adhesion process. Thus, in some studies, it was found that proteins adhere preferentially to hydrophilic surfaces, while in others, to hydrophobic surfaces. The in vitro studies regarding the adhesion of albumin showed that it presents affinity especially for hydrophobic surfaces. This behavior is a consequence of distortion induced by the interaction of the hydrophobic core with the hydrophilic surface [59]. In addition to the mentioned factors, the involvement of the surface charge must also be taken into account, because it can produce attraction or repulsion of the plasma proteins. As for albumin, due to the inhomogeneous charge distribution on the surface, its adsorption is possible on both positively and negatively charged surfaces.

Table 5. Spreading work of water ($W_{s,w}$), blood components ($W_{s,rbc}$ and $W_{s,p}$) and plasma proteins ($W_{s,albumin}$, $W_{s,fibrinogen}$, and $W_{s,IgG}$) for PI-2 and PI-2/S(1–3) hybrid materials according to Equation (6).

Sample	$W_{s,w}$	$W_{s,rbc}$	$W_{s,p}$	$W_{s,Albumin}$	$W_{s,Fibrinogen}$	$W_{s,IgG}$
PI-2	−72.28	−2.46	−120.41	−52.46	−10.65	−28.41
PI-2/S1	−51.54	−0.99	−98.89	−42.55	−7.70	−22.83
PI-2/S2	−28.82	3.19	−82.84	−28.82	−2.95	−14.12
PI-2/S3	−27.08	−0.37	−83.89	−30.00	−6.24	−16.68

$W_{s,w}$: work on spreading of water; $W_{s,rbc}$: work on spreading of red blood cells; $W_{s,p}$: work on spreading of platelets; $W_{s,albumin}$: work on spreading of albumin; $W_{s,fibrinogen}$: work on spreading of fibrinogen, $W_{s,IgG}$: work on spreading of immunoglobulin G.

The results of these mathematical approaches can be taken into account in future studies because they predict the biocompatibility of PI-2/spirulina hybrid materials and also their ability to be successfully used as biomaterials in the medical field.

3.5. Water Uptake

The ability of polymeric materials to absorb water or fluids akin to human body fluids is a crucial aspect in various applications [60]. This water uptake in polyimides is influenced by several factors, including the chemical structure and the introduction of functional groups [61]. Therefore, the wetting capacity of these films was thoroughly investigated, with a focus on the type of polyimide utilized and the concentration of spirulina incorporated. As depicted in Figure 7, the PI-2 films loaded with spirulina exhibited maximum water uptake, with the degree of absorption reaching peak values

of 150% for PI-2 and 450% for PI-2/S3. This heightened water uptake of PI-2 can be attributed to the augmentation of free volume within the polymer matrix, facilitating the accommodation of water molecules. Furthermore, the swelling behavior in water showed an incremental trend until reaching a saturation point, with the PI-2 films achieving a constant value after a certain duration. The absorption kinetics depicted an initial rapid increase within the first 25 min, followed by a gradual rise over approximately 50 min, culminating in equilibrium at approximately 60 min. Notably, the polyimide film with spirulina (PI-2/S3) demonstrated the highest degree of water absorption, reaching a remarkable value of 450%. This enhanced absorption capacity underscores the synergistic effects of spirulina incorporation, which likely facilitates increased water retention within the polymer matrix. Overall, these findings provide valuable insights into the water absorption behavior of polyimide films loaded with spirulina, shedding light on their potential suitability for applications requiring controlled hydration or fluid management, such as biomedical devices or drug delivery systems.

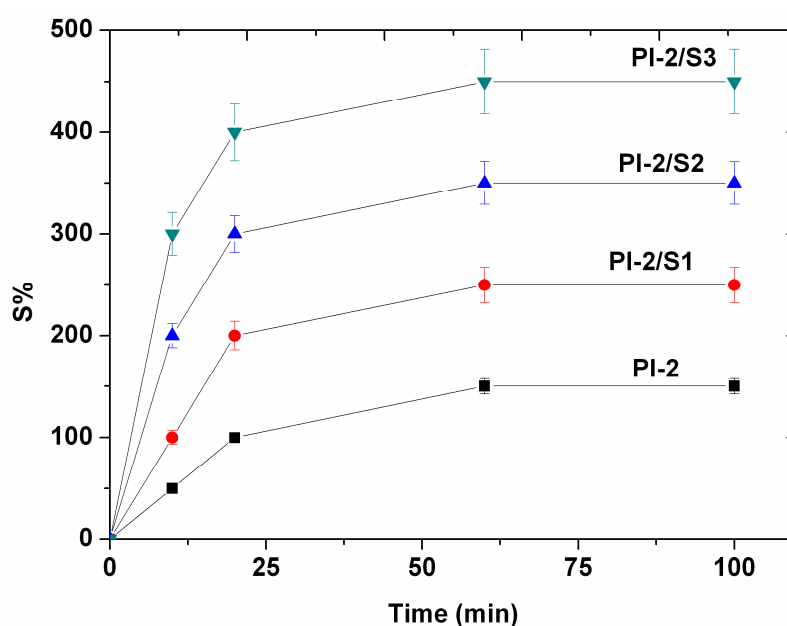


Figure 7. Water uptake for PI-2 and PI-2/S(1–3) hybrid materials.

4. Conclusions

This study successfully incorporated spirulina powder into a polyimide (PI-2) matrix, achieving a homogeneous dispersion of spirulina particles. This integration was characterized by SEM imaging, revealing a tightly bound interface between spirulina and the PI-2 matrix, indicating robust interfacial adhesion. Profilometry and Raman spectroscopy techniques were employed to analyze the surface characteristics of the hybrid materials. The results demonstrated variations in surface roughness and chemistry upon spirulina incorporation, highlighting the ability to tailor surface properties for specific applications. Contact angle measurements indicated alterations in the wettability of the hybrid materials, with increased hydrophilicity observed with spirulina incorporation. This modification holds implications for potential biomedical applications, where surface characteristics play a critical role in biocompatibility. The study assessed the interaction of blood components (red blood cells, platelets, and plasma proteins) with the hybrid materials. Results suggested potential biocompatibility, with variations in adhesion behavior observed for different blood components. This assessment is crucial for evaluating the suitability of the hybrid materials for biomedical applications. Water uptake studies revealed enhanced absorption capacity in PI-2 films loaded with spirulina, indicating potential suitability for applications requiring controlled hydration. This aspect holds significance for applications such as biomedical devices or drug delivery systems. Overall, the study provides valuable

insights into the development of polyimide–spirulina hybrid materials with enhanced functionality for biomedical applications. Future research endeavors could focus on further optimizing these hybrid materials and exploring their specific performance in diverse biomedical contexts, aiming to translate these findings into practical applications.

Author Contributions: Conceptualization, D.S. and M.A.; methodology, D.S.; validation, M.A., A.M.I. and A.M.D.; investigation, D.R.; data curation, D.S.; writing—original draft preparation, D.S. and M.A.; writing—review and editing, D.S. and M.A. All authors have read and agreed to the published version of the manuscript.

Funding: This research received no external funding.

Data Availability Statement: Data will be available upon request.

Conflicts of Interest: The authors declare no conflicts of interest.

References

1. Egbo, M.K. A fundamental review on composite materials and some of their applications in biomedical engineering. *J. King Saud Univ.-Eng. Sci.* **2021**, *33*, 557–568. [[CrossRef](#)]
2. Sharma, H.; Kumar, A.; Rana, S.; Sahoo, N.G.; Jamil, M.; Kumar, R.; Sharma, S.; Li, C.; Kumar, A.; Eldin, S.M.; et al. Critical review on advancements on the fiber-reinforced composites: Role of fiber/matrix modification on the performance of the fibrous composites. *J. Mater. Res. Technol.* **2023**, *26*, 2975–3002. [[CrossRef](#)]
3. Wu, C.; Xu, F.; Wang, H.; Liu, H.; Yan, F.; Ma, C. Manufacturing Technologies of Polymer Composites—A Review. *Polymers* **2023**, *15*, 712. [[CrossRef](#)] [[PubMed](#)]
4. Lazăr, S.; Dobrotă, D.; Breaz, R.-E.; Racz, S.-G. Eco-Design of Polymer Matrix Composite Parts: A Review. *Polymers* **2023**, *15*, 3634. [[CrossRef](#)]
5. Tri-Dung, N. (Ed.) Introduction to Composite Materials. In *Composite and Nanocomposite Materials*; IntechOpen: Rijeka, Croatia, 2020; Chapter 1.
6. Aflori, M.; Miron, C.; Dobromir, M.; Drobotă, M. Bactericidal effect on Foley catheters obtained by plasma and silver nitrate treatments. *High Perform. Polym.* **2015**, *27*, 655–660. [[CrossRef](#)]
7. Ramakrishna, S.; Mayer, J.; Wintermantel, E.; Leong, K.W. Biomedical applications of polymer-composite materials: A review. *Compos. Sci. Technol.* **2001**, *61*, 1189–1224. [[CrossRef](#)]
8. Zagho, M.M.; Hussein, E.A.; Elzatahry, A.A. Recent Overviews in Functional Polymer Composites for Biomedical Applications. *Polymers* **2018**, *10*, 739. [[CrossRef](#)] [[PubMed](#)]
9. Ramesh, M.; Manickam, T.S.; Arockiasamy, F.S.; Ponnusamy, B.; Senthilraj, S.; Chellamuthu, D.; Palanisamy, P. Revolutionizing Biomedicine: A Comprehensive Review of Polymer Composite Materials. *Eng. Proc.* **2024**, *61*, 17. [[CrossRef](#)]
10. Chiriac, A.I.; Pastor, F.I.J.; Popa, V.I.; Aflori, M.; Ciolacu, D. Changes of supramolecular cellulose structure and accessibility induced by the processive endoglucanase Cel9B from *Paenibacillus barcinonensis*. *Cellulose* **2014**, *21*, 203–219. [[CrossRef](#)]
11. Lunetto, V.; Galati, M.; Settineri, L.; Iuliano, L. Sustainability in the manufacturing of composite materials: A literature review and directions for future research. *J. Manuf. Process.* **2023**, *85*, 858–874. [[CrossRef](#)]
12. Ogbonna, V.E.; Popoola, A.P.I.; Popoola, O.M.; Adeosun, S.O. A review on polyimide reinforced nanocomposites for mechanical, thermal, and electrical insulation application: Challenges and recommendations for future improvement. *Polym. Bull.* **2020**, *79*, 1–33. [[CrossRef](#)]
13. Lee, S.; Eom, Y.; Kim, B.J.; Mochida, I.; Yoon, S.H.; Kim, B.C. The thermotropic liquid crystalline behavior of mesophase pitches with different chemical structures. *Carbon* **2015**, *81*, 694–701. [[CrossRef](#)]
14. Liaw, D.J.; Wang, K.L.; Huang, Y.C.; Lee, K.R.; Lai, J.Y.; Ha, C.S. Advanced polyimide materials: Syntheses, physical properties and applications. *Prog. Polym. Sci.* **2012**, *37*, 907–974. [[CrossRef](#)]
15. Serbezeanu, D.; Vlad-Bubulac, T.; Rusu, D.; Grădișteanu Pircalabioru, G.; Samoilă, I.; Dinescu, S.; Aflori, M. Functional Polyimide-Based Electrospun Fibers for Biomedical Application. *Materials* **2019**, *12*, 3201. [[CrossRef](#)] [[PubMed](#)]
16. Constantin, C.P.; Aflori, M.; Damian, R.F.; Rusu, R.D. Biocompatibility of Polyimides: A Mini-Review. *Materials* **2019**, *12*, 3166. [[CrossRef](#)]
17. Cuello, E.A.; Mulko, L.E.; Barbero, C.A.; Acevedo, D.F.; Yslas, E.I. Development of micropatterning polyimide films for enhanced antifouling and antibacterial properties. *Colloids Surf. B Biointerfaces* **2020**, *188*, 110801. [[CrossRef](#)]
18. Radu Dan, R.; Marc, J.M.A. New High-Performance Materials: Bio-Based, Eco-Friendly Polyimides. In *Polyimide for Electronic and Electrical Engineering Applications*; Sombel, D., Ed.; IntechOpen: Rijeka, Croatia, 2020; Chapter 15.
19. Ogbonna, V.E.; Popoola, P.I.; Popoola, O.M.; Adeosun, S.O. A review on recent advances on improving polyimide matrix nanocomposites for mechanical, thermal, and tribological applications: Challenges and recommendations for future improvement. *J. Thermoplast. Compos. Mater.* **2023**, *36*, 836–865. [[CrossRef](#)]
20. Gouzman, I.; Grossman, E.; Verker, R.; Atar, N.; Bolker, A.; Eliaz, N. Advances in Polyimide-Based Materials for Space Applications. *Adv. Mater.* **2019**, *31*, 1807738. [[CrossRef](#)]

21. Ma, P.; Dai, C.; Wang, H.; Li, Z.; Liu, H.; Li, W.; Yang, C. A review on high temperature resistant polyimide films: Heterocyclic structures and nanocomposites. *Compos. Commun.* **2019**, *16*, 84–93. [[CrossRef](#)]
22. Ogbonna, V.E.; Popoola, P.; Popoola, O.M.; Adeosun, S.O. Recent progress on improving the mechanical, thermal and electrical conductivity properties of polyimide matrix composites from nanofillers perspective for technological applications. *J. Polym. Eng.* **2021**, *41*, 768–787. [[CrossRef](#)]
23. Hamciuc, C.; Vlad-Bubulac, T.; Bercea, M.; Suflet, D.M.; Doroftei, F.; Rîmbu, C.M.; Enache, A.A.; Kalvachev, Y.; Todorova, T.; Butnaru, M.; et al. Electrospun Copoly (ether imide) Nanofibers Doped with Silver-Loaded Zeolite as Materials for Biomedical Applications. *ACS Appl. Polym. Mater.* **2022**, *4*, 6080–6091. [[CrossRef](#)]
24. Hamciuc, C.; Lisa, G.; Serbezeanu, D.; Grădinaru, L.M.; Asăndulesa, M.; Tudorachi, N.; Vlad-Bubulac, T. Tailoring Thermal and Electrical Properties of Jeffamine Segmented Polyetherimide Composite Films Containing BaTiO₃ particles. *Polymers* **2022**, *14*, 4715. [[CrossRef](#)]
25. Serbezeanu, D.; Popa, A.M.; Sava, I.; Carja, I.D.; Amberg, M.; Rossi, R.M.; Fortunato, G. Design and synthesis of polyimide—Gold nanofibers with tunable optical properties. *Eur. Polym. J.* **2015**, *64*, 10–20. [[CrossRef](#)]
26. Ma, J.; Liu, X.; Wang, R.; Lu, C.; Wen, X.; Tu, G. Research Progress and Application of Polyimide-Based Nanocomposites. *Nanomaterials* **2023**, *13*, 656. [[CrossRef](#)]
27. Jaji, N.D.; Othman, M.B.H.; Lee, H.L.; Hussin, M.H.; Md Akil, H.; Aljunid Merican, Z.M.; Omar, M.F. Polyimide–nickel nanocomposites fabrication, properties, and applications: A review. *Rev. Adv. Mater. Sci.* **2023**, *62*, 20230113. [[CrossRef](#)]
28. Bortolini, D.G.; Maciel, G.M.; Fernandes, I.d.A.A.; Pedro, A.C.; Rubio, F.T.V.; Branco, I.G.; Haminiuk, C.W.I. Functional properties of bioactive compounds from *Spirulina* spp.: Current status and future trends. *Food Chem.* **2022**, *5*, 100134. [[CrossRef](#)]
29. Fratelli, C.; Nunes, M.C.; De Rosso, V.V.; Raymundo, A.; Braga, A.R.C. Spirulina and its residual biomass as alternative sustainable ingredients: Impact on the rheological and nutritional features of wheat bread manufacture. *Sec. Food Charact.* **2023**, *3*, 1258219. [[CrossRef](#)]
30. AlFadhly, N.K.Z.; Alhelfi, N.; Altemimi, A.B.; Verma, D.K.; Cacciola, F.; Narayanankutty, A. Trends and Technological Advancements in the Possible Food Applications of Spirulina and Their Health Benefits: A Review. *Molecules* **2022**, *27*, 5584. [[CrossRef](#)]
31. Sahin, B.; Hosoglu, M.I.; Guner, O.; Karagul-Yuceer, Y. Nutrition and flavor analysis of Spirulina through co-fermentation with *Lactobacillus acidophilus* and *Kluyveromyces marxianus* and its effect on attenuating metabolic associated fatty liver disease. *J. Funct. Foods* **2024**, *116*, 106149.
32. Guan, F.; Fu, G.; Ma, Y.; Zhou, L.; Li, G.; Sun, C.; Zhang, T. Spirulina polysaccharide-based prebiotic foods preparations—A promising approach for modulating gut microbiota and improving health. *J. Funct. Foods* **2024**, *116*, 106158. [[CrossRef](#)]
33. Trotta, T.; Porro, C.; Cianciulli, A.; Panaro, M.A. Beneficial Effects of Spirulina Consumption on Brain Health. *Nutrients* **2022**, *14*, 676. [[CrossRef](#)]
34. Bermejo-Bescós, P.; Piñero-Estrada, E.; del Fresno, Á.M.V. Neuroprotection by Spirulina platensis protean extract and phycocyanin against iron-induced toxicity in SH-SY5Y neuroblastoma cells. *Toxicol. Vitro.* **2008**, *22*, 1496–1502. [[CrossRef](#)]
35. Dmytryk, A.; Saeid, A.; Chojnacka, K. Biosorption of Microelements by *Spirulina*: Towards Technology of Mineral Feed Supplements. *Sci. World J.* **2014**, *2014*, 356328. [[CrossRef](#)]
36. Taiti, C.; Di Vito, M.; Di Mercurio, M.; Costantini, L.; Merendino, N.; Sanguinetti, M.; Bugli, F.; Garzoli, S. Detection of Secondary Metabolites, Proximate Composition and Bioactivity of Organic Dried Spirulina (*Arthrospira platensis*). *Appl. Sci.* **2024**, *14*, 67. [[CrossRef](#)]
37. Schmatz, D.A.; da Silva Uebel, L.; Kuntzler, S.G.; Dora, C.L.; Vieira Costa, J.A.; de Moraes, M.G. Scaffolds Containing *Spirulina* sp. LEB 18 Biomass: Development, Characterization and Evaluation of In Vitro Biodegradation. *J. Nanosci. Nanotechnol.* **2016**, *16*, 1050–1059. [[CrossRef](#)] [[PubMed](#)]
38. de Moraes, M.G.; Vaz, B.d.S.; de Moraes, E.G.; Costa, J.A. Biological Effects of *Spirulina* (*Arthrospira*) Biopolymers and Biomass in the Development of Nanostructured Scaffolds. *BioMed Res. Int.* **2014**, *2014*, 762705. [[CrossRef](#)] [[PubMed](#)]
39. Slepickova Kasalkova, N.; Slepicka, P.; Kolska, Z.; Svorcik, V. Wettability and Other Surface Properties of Modified Polymers. In *Wetting and Wettability*; Mahmood, A., Ed.; IntechOpen: Rijeka, Croatia, 2015; Chapter 12.
40. Liu, X.; He, J. Superhydrophilic and Antireflective Properties of Silica Nanoparticle Coatings Fabricated via Layer-by-Layer Assembly and Postcalcination. *J. Phys. Chem. C* **2009**, *113*, 148–152. [[CrossRef](#)]
41. Cheng, X.; Ling, P.; Iqbal, M.S.; Liu, F.; Xu, J.; Wang, X. Water adsorption properties of microalgae powders: Thermodynamic analysis and structural characteristics. *J. Stored Prod. Res.* **2023**, *101*, 102093. [[CrossRef](#)]
42. Rankl, M.; Laib, S.; Seeger, S. Surface tension properties of surface-coatings for application in biodiagnostics determined by contact angle measurements. *Colloids Surf. B Biointerfaces* **2003**, *30*, 177–186. [[CrossRef](#)]
43. Asadpour, S.; Ai, J.; Davoudi, P.; Ghorbani, M.; Jalali Monfared, M.; Ghanbari, H. In vitro physical and biological characterization of biodegradable elastic polyurethane containing ferulic acid for small-caliber vascular grafts. *Biomed. Mater.* **2018**, *13*, 035007. [[CrossRef](#)]
44. Kwok, S.C.H.; Wang, J.; Chu, P.K. Surface energy, wettability, and blood compatibility phosphorus doped diamond-like carbon films. *Diam. Relat. Mater.* **2005**, *14*, 78–85. [[CrossRef](#)]
45. Agathopoulos, S.; Nikolopoulos, P. Wettability and interfacial interactions in bioceramic-body-liquid systems. *J. Biomed. Mater. Res.* **1995**, *29*, 421–429. [[CrossRef](#)]

46. van Oss, C.J. Surface properties of fibrinogen and fibrin. *J. Protein Chem.* **1990**, *9*, 487–491. [[CrossRef](#)]
47. van Oss, C.J. Long-range and short-range mechanisms of hydrophobic attraction and hydrophilic repulsion in specific and aspecific interactions. *J. Mol. Recognit.* **2003**, *16*, 177–190. [[CrossRef](#)] [[PubMed](#)]
48. Bayat, A.; Ebrahimi, M.; Moshfegh, A.Z. Correlation between surface roughness and hydrophobicity of GLAD RF sputtered PTFE/W/Glass nanorod thin films. *Vacuum* **2014**, *101*, 279–282. [[CrossRef](#)]
49. Vijayanand, K.; Pattanayak, D.K.; Mohan, T.R.; Banerjee, R. Interpreting Blood-Biomaterial Interactions from Surface Free Energy and Work of Adhesion. *Trends Biomater. Artif. Organs* **2005**, *18*, 73–83.
50. Van Oss, C.J. *Interfacial Forces in Aqueous Media*; CRC Press: Boca Raton, FL, USA, 2006.
51. Zhang, J.; Xu, B.; Zhang, P.; Cai, M.; Li, B. Effects of surface roughness on wettability and surface energy of coal. *Front. Earth Sci.* **2023**, *10*, 1054896. [[CrossRef](#)]
52. Wang, X.; Zhang, Q. Role of surface roughness in the wettability, surface energy and flotation kinetics of calcite. *Powder Technol.* **2020**, *371*, 55–63. [[CrossRef](#)]
53. Wenzel, R.N. Resistance of Solid Surfaces to Wetting by Water. *Ind. Eng. Chem.* **1936**, *28*, 988–994. [[CrossRef](#)]
54. Silvia, I.; Anca, F. Biocompatibility and Antimicrobial Activity of Some Quaternized Polysulfones. In *A Search for Antibacterial Agents*; Varaprasad, B., Ed.; IntechOpen: Rijeka, Croatia, 2012; Chapter 13.
55. Filimon, A.; Dobos, A.M.; Musteata, V. New perspectives on development of polysulfones/cellulose derivatives based ionic-exchange membranes: Dielectric response and hemocompatibility study. *Carbohydr. Polym.* **2019**, *226*, 115300. [[CrossRef](#)]
56. Zheng, K.; Kapp, M.; Boccaccini, A.R. Protein interactions with bioactive glass surfaces: A review. *Appl. Mater. Today* **2019**, *15*, 350–371. [[CrossRef](#)]
57. Toffoli, A.; Parisi, L.; Bianchi, M.G.; Lumetti, S.; Bussolati, O.; Macaluso, G.M. Thermal treatment to increase titanium wettability induces selective proteins adsorption from blood serum thus affecting osteoblasts adhesion. *Mater. Sci. Eng. C Mater. Biol. Appl.* **2020**, *107*, 110250. [[CrossRef](#)] [[PubMed](#)]
58. Ferraris, S.; Cazzola, M.; Peretti, V.; Stella, B.; Spriano, S. Zeta Potential Measurements on Solid Surfaces for in Vitro Biomaterials Testing: Surface Charge, Reactivity Upon Contact with Fluids and Protein Absorption. *Front. Bioeng. Biotechnol.* **2018**, *6*, 60. [[CrossRef](#)]
59. Zelzer, M.; Albutt, D.; Alexander, M.R.; Russell, N.A. The Role of Albumin and Fibronectin in the Adhesion of Fibroblasts to Plasma Polymer Surfaces. *Plasma Process. Polym.* **2012**, *9*, 149–156. [[CrossRef](#)]
60. Mignon, A.; De Belie, N.; Dubruel, P.; Van Vlierberghe, S. Superabsorbent polymers: A review on the characteristics and applications of synthetic, polysaccharide-based, semi-synthetic and ‘smart’ derivatives. *Eur. Polym. J.* **2019**, *117*, 165–178. [[CrossRef](#)]
61. Seo, J.; Cho, K.-Y.; Han, H. Dependence of water sorption in polyimides on the internal linkage in the diamine component. *Polym. Degrad. Stab.* **2001**, *74*, 133–137. [[CrossRef](#)]

Disclaimer/Publisher’s Note: The statements, opinions and data contained in all publications are solely those of the individual author(s) and contributor(s) and not of MDPI and/or the editor(s). MDPI and/or the editor(s) disclaim responsibility for any injury to people or property resulting from any ideas, methods, instructions or products referred to in the content.